

Notes

Clusters $[\{\text{Pt}(\text{diphosphine})(\text{isocyanide})\}_2\text{Pt}]^{2+}$ Recharacterized as $[\{\text{Pt}(\text{diphosphine})(\text{isocyanide})\}_2\text{Hg}]^{2+}$

Tomoaki Tanase,[†] Yasuhiro Yamamoto,^{*,†} and R. J. Puddephatt[‡]

Departments of Chemistry, Faculty of Science, Toho University, Miyama 2-2-1, Funabashi, Chiba 274, Japan, and University of Western Ontario, London, Canada N6A 5B7

Received December 11, 1995[Ⓢ]

Summary: The clusters already reported as $\{\text{Pt}(\text{diphos})(\text{RNC})\}_2\text{Pt}(\text{PF}_6)_2$, (diphos = *cis*-Ph₂PCH=CHPPh₂, Ph₂P(CH₂)₃PPh₂, or ^tBu₂P(CH₂)₂P^tBu₂; R = 2,6-xylyl or 2,4,6-mesityl) have been recharacterized to be the Pt–Hg–Pt mixed-metal clusters $[\{\text{Pt}(\text{diphos})(\text{RNC})\}_2\text{Hg}](\text{PF}_6)_2$ on the basis of metal analysis and the reevaluation of ³¹P{¹H} NMR spectra and X-ray crystallographic structures.

We have studied the electrochemical reduction of platinum and palladium complexes containing diphosphines and isocyanides, in which a new types of triplatinum complex having a naked platinum center, $[\{\text{Pt}(\text{diphos})(\text{RNC})\}_2\text{Pt}](\text{PF}_6)_2$, have been reported as the first examples of 40-electron triplatinum clusters, where diphos is *cis*-Ph₂PCH=CHPPh₂ (dppen) (**13**), Ph₂P(CH₂)₃PPh₂ (dppp) (**14**), or ^tBu₂P(CH₂)₂P^tBu₂ (dtbpe) (**15**).^{1–3} Recently, we considered that the clusters **13–15** may be incorrectly formulated and that they may have the formula $[\{\text{Pt}(\text{diphos})(\text{RNC})\}_2\text{Hg}](\text{PF}_6)_2$, on the basis of a new interpretation of their ³¹P{¹H} NMR spectra. This suggestion is not inconsistent with our results of X-ray, EXAFS, and other spectroscopic analyses for **13–15** since platinum and mercury have similar atomic weights. We have immediately made an analysis of the metal ions, and here we wish to make a correction and to describe recharacterization of the clusters **13–15** as $[\{\text{Pt}(\text{diphos})(\text{RNC})\}_2\text{Hg}](\text{PF}_6)_2$.

Experimental Section

Synthetic procedures, analytical data, and UV–vis, IR, and ¹H NMR and ³¹P{¹H} NMR spectral data for $[\{\text{Pt}(\text{dppen})(\text{RNC})\}_2\text{Hg}](\text{PF}_6)_2$ (**13a**·CH₂Cl₂, R = Xyl; **13b**·CH₂Cl₂, R = Mes), $[\{\text{Pt}(\text{dppp})(\text{RNC})\}_2\text{Hg}](\text{PF}_6)_2$ (**14a**, R = Xyl; **14b**, R = Mes), and $[\{\text{Pt}(\text{dtbpe})(\text{XylNC})\}_2\text{Hg}](\text{PF}_6)_2$ (**15a**) have already been cited in ref 2.³ The following abbreviations are used: dppen = *cis*-1,2-bis(diphenylphosphine)ethene, dppp = 1,3-bis(diphenylphosphino)propane, dtbpe = 1,2-bis(di-*tert*-butylphosphino)ethane, Xyl = 2,6-xylyl, Mes = 2,4,6-mesityl.

[†] Toho University.

[‡] University of Western Ontario.

[Ⓢ] Abstract published in *Advance ACS Abstracts*, February 1, 1996.

(1) Tanase, T.; Kudo, Y.; Ohno, M.; Kobayashi, K.; Yamamoto, Y. *Nature* **1990**, *344*, 526.

(2) Tanase, T.; Ukaji, H.; Kudo, Y.; Ohno, M.; Kobayashi, K.; Yamamoto, Y. *Organometallics* **1994**, *13*, 1374.

(3) The same compound numbers as in ref 2 are used in this report.

Table 1. Structural Parameters of Clusters **13a, **14a**, and **15a****

	13a	14a	15a
Pt–Hg, Å	2.615(1)	2.640 ^a	2.6409(9)
Pt–P _{ax} , Å ^b	2.298(4)	2.31 ^a	2.335(4)
Pt–P _{eq} , Å ^b	2.260(4)	2.29 ^a	2.307(4)
Pt–C, Å	1.95(2)	1.90 ^a	1.93(1)
N–C, Å	1.16(2)	1.17 ^a	1.17(2)
Pt–Hg–Pt, deg	163.69(5)	178.21(9)	167.26(4)
Hg–Pt–P _{ax} , deg	166.0(1)	173.0 ^a	173.3(1)
Hg–Pt–P _{eq} , deg	86.6(1)	87.7 ^a	94.0(1)
Hg–Pt–C, deg	81.4(4)	84 ^a	78.7(4)
P–Pt–P, deg	86.1(2)	93.2 ^a	88.6(2)
Pt–C–N, deg	178(1)	173 ^a	179(1)
C–N–C, deg	167(2)	170 ^a	171(1)
θ, deg ^d	59	85	72

^a Average value. ^b The P_{ax} and P_{eq} atoms sit in the *trans* and *cis* positions, respectively, to the Pt–Hg bond. ^c The dihedral angle between the coordination planes around the outer platinum atoms.

The ratio of Pt:Hg for **13a**·CH₂Cl₂ was determined to be 2.0:0.9 by inductively coupled plasma-atomic emissions spectroscopy (ICP) on a Jobin Yvan Model JY 38S. The absolute observed values for Pt and Hg are 17.4% and 7.6%, respectively, which are smaller by ~2% than the calculated values (19.3% and 9.9%) probably due to the small amount of sample used in the measurement.

X-ray Crystallographic Analyses of **13a·2CH₃CN, **14a**, and **15a**.** Crystal data and experimental procedures were reported in ref 2. Structure refinements of **13a**·2CH₃CN, **14a**, and **15a** were performed with the Hg scattering factors for the central metal by similar procedures as described before. Listings of crystallographic data, final atomic parameters, and bond distances and angles are supplied as Supporting Information.

Molecular Orbital Calculations. Extended Hückel MO calculations were carried out by using parameters of the Coulomb integrals and the orbital exponents taken from ref 4. For the Pt and Hg d functions, a double-ζ expansion was used. Geometrical assumptions were derived from the crystal structure of **14a**: Pt–Hg = 2.64 Å, Pt–P = 2.30 Å, Pt–C = 1.97 Å, N–C = 1.15 Å, P–H = 1.42 Å, N–H = 1.01 Å; Pt–Hg–Pt = 180°, Hg–Pt–P_{ax} = 180°, Hg–Pt–P_{eq} = 90°, Hg–Pt–C = 90°.

(4) (a) Dedieu, A.; Hoffmann, R. *J. Am. Chem. Soc.* **1978**, *100*, 2074.

(b) Underwood, D. J.; Hoffmann, R.; Tatsumi, K.; Nakamura, A.; Yamamoto, Y. *J. Am. Chem. Soc.* **1985**, *107*, 5968.

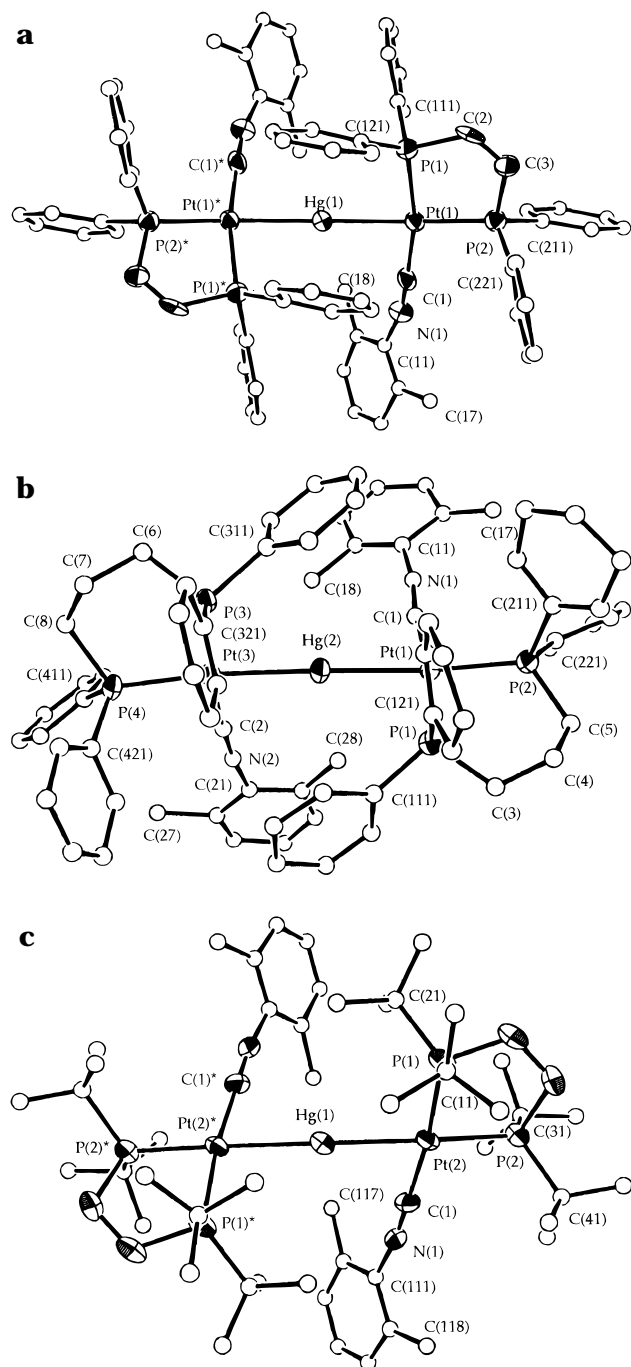


Figure 1. Perspective drawings of the complex cations of (a) **13a**, $[\{\text{Pt}(\text{dppen})(\text{XylNC})\}_2\text{Hg}]^{2+}$, (b) **14a**, $[\{\text{Pt}(\text{dppp})(\text{XylNC})\}_2\text{Hg}]^{2+}$, and (c) **15a**, $[\{\text{Pt}(\text{dtbpe})(\text{XylNC})\}_2\text{Hg}]^{2+}$.

Results and Discussion

Our previous paper² did not report the analytical data of the metal ions for the triplatinum clusters **13–15** because of their low yields, limitation of the synthetic scale in the electrochemical method, and the difficulty of obtaining pure samples in large amounts. The metal analysis, however, is crucial to discriminate in the cluster structures between the Pt–Pt–Pt and the Pt–Hg–Pt cores. The ratio of Pt:Hg in **13a** was determined to be 2.0:0.9 by ICP emission spectroscopy. On the basis of the metal analysis as well as extensive analytical and spectroscopic data already reported, it was concluded that the clusters **13–15** are formulated as

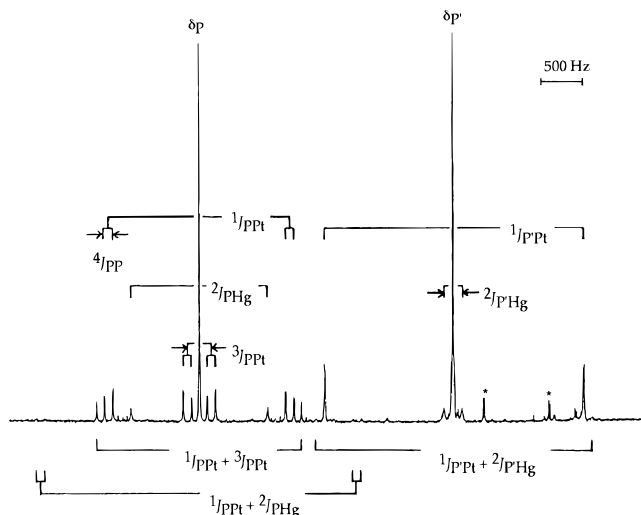


Figure 2. $^{31}\text{P}\{^1\text{H}\}$ NMR spectrum of $[\{\text{Pt}(\text{dppen})(\text{XylNC})\}_2\text{Hg}](\text{PF}_6)_2$ (**13a**).

Table 2. $^{31}\text{P}\{^1\text{H}\}$ NMR Spectral Data for **13a** and **15a**^a

	13a ^b	15a
δ_P , ppm	92.6	126.7
$\delta_{P'}$, ppm	62.5	102.0
$^1J_{\text{PPt}}$, Hz	2157	2081
$^1J_{P'\text{Pt}}$, Hz	3090	3126
$^2J_{\text{PHg}}$, Hz	1632	1505
$^2J_{P'\text{Hg}}$, Hz	218	117
$^3J_{\text{PPt}}$, Hz	286	273
$^3J_{P'\text{Pt}}$, Hz	29	12
$^2J_{\text{PP}'}$, Hz	10	5
$^4J_{\text{PP}}$, Hz	100	89

^a Measured at 63.32 MHz in CD_2Cl_2 at room temperature. ^b See Figure 2.

$[\{\text{Pt}(\text{diphos})(\text{RNC})\}_2\text{Hg}](\text{PF}_6)_2$. The Pt–Hg–Pt mixed-metal clusters **13–15** are not coordinatively unsaturated and have 42 valence electrons. The mercury atom is assumed to be derived from the cathode (mercury pool electrode) in electrolysis. The structure of $[\{\text{Pt}(\text{diphos})(\text{RNC})\}_2\text{Hg}](\text{PF}_6)_2$ is consistent with the synthetic scheme in ref 2 as well as the $^{31}\text{P}\{^1\text{H}\}$ NMR spectroscopic, EXAFS, and X-ray crystallographic data and extended Hückel molecular orbital calculations (*vide infra*).

The X-ray crystal structures of **13a**, **14a**, and **15a** were refined with the Pt–Hg–Pt model. ORTEP plots of the complex cations of **13a**, **14a**, and **15a** are illustrated in Figure 1, and some selected structural parameters are summarized in Table 1. The Pt–Hg bond lengths of 2.615(1) Å (**13a**), 2.640 Å (average) (**14a**), and 2.6409(9) Å (**15a**) are considerably shorter than those found in the Pt–Hg–Pt A-frame complex $[\text{Pt}_2(\mu\text{-HgCl}_2)(\text{dppm})_2\text{Cl}_2]$ (dppm = bis(diphenylphosphino)methane) (average 2.709 Å)⁵ and in the Pt_6Hg and Pt_6Hg_2 clusters (2.878–3.084 Å).^{6–8} Other peripheral

(5) Sharp, P. R. *Inorg. Chem.* **1986**, *25*, 4185.

(6) Albinati, A.; Moor, A.; Pregosin, P. S.; Venanzi, L. M. *J. Am. Chem. Soc.* **1982**, *104*, 7672.

(7) Yamamoto, Y.; Yamazaki, H.; Sakurai, T. *J. Am. Chem. Soc.* **1982**, *104*, 2329.

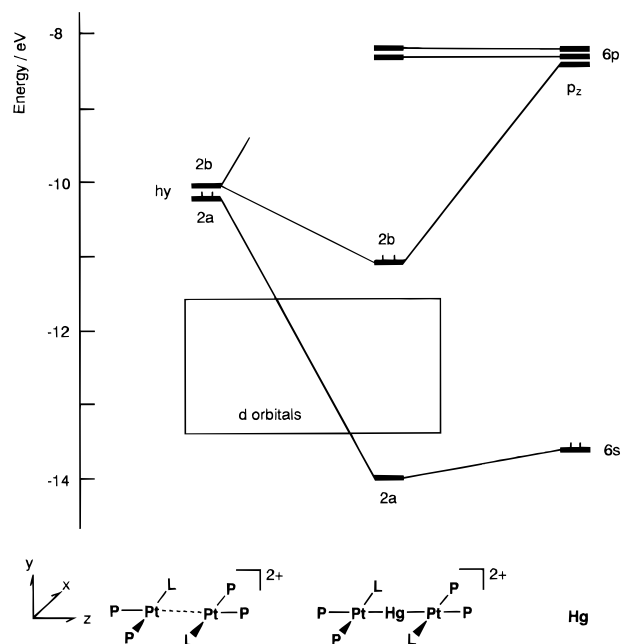


Figure 3. Interaction diagram for $[\{\text{Pt}(\text{PH}_3)_2(\text{HNC})\}_2\text{Hg}]^{2+}$ (**I**) in terms of $[\text{Pt}(\text{PH}_3)_2(\text{HNC})\cdots\text{Pt}(\text{PH}_3)_2(\text{HNC})]^{2+}$ and Hg^0 .

structures of **13a**, **14a**, and **15a** are almost the same as previously reported.²

The $^{31}\text{P}\{^1\text{H}\}$ NMR spectrum of $[\{\text{Pt}(\text{dppen})(\text{XylNC})\}_2\text{Hg}](\text{PF}_6)_2$ (**13a**) is shown in Figure 2, and the spectral data for **13a** and $[\{\text{Pt}(\text{dtbpe})(\text{XylNC})\}_2\text{Hg}](\text{PF}_6)_2$ (**15a**) are listed in Table 2. The spectral pattern is in good

(8) Tanase, T.; Horiuchi, T.; Yamamoto, Y.; Kobayashi, K. *J. Organomet. Chem.* **1992**, *440*, 1.

accord with the Pt–Hg–Pt structure; in particular, weak satellites due to $^2J_{\text{PtHg}}$ coupling, whose intensities are less than half of those due to $^1J_{\text{PtPt}}$ or $^3J_{\text{PtPt}}$ coupling, are well explained in terms of the natural abundance of ^{199}Hg (16.8%), which is about half that of ^{195}Pt (33.8%).

In the Fourier transforms of EXAFS oscillations of **13a–15a** (after the Pt L_3 edge),⁹ the outer peak around 2.7 Å (before phase-shift correction) should be assigned to the back-scattering contributions of the neighboring mercury atom, although the Pt and Hg scattering atoms are hardly distinguished in the present EXAFS analyses.

Finally, extended Hückel molecular orbital calculations were reexamined by using a model $[\{\text{Pt}(\text{PH}_3)_2(\text{CNH})\}_2\text{Hg}]^{2+}$ (**I**). An orbital energy interaction diagram for formation of **I** is shown in Figure 3. The diagram is essentially similar to that for $[\{\text{Pt}(\text{PH}_3)_2(\text{CNH})\}_2\text{Pt}]^{2+}$ (**II**), except that the LUMO in **II** is occupied by two extra electrons in **I**. Consequently, all the M–M bonding orbitals (2b, 2a) are occupied and the HOMO–LUMO gap is large enough (2.52 eV) in the Pt–Hg–Pt model (**I**), leading to a normal and stable metal–metal-bonded structure.

Supporting Information Available: Listings of crystallographic data, final atomic parameters, and bond distances and angles for **13a**, **14a**, and **15a** (31 pages). Ordering information is given on any current masthead page.

OM9509498

(9) See Figure 5 in ref 2.